

***In Situ* and Time Resolved Synchrotron X-ray Diffraction Investigation of Solvothermal Synthesis of Mesoporous TiO₂ Beads**

Fang Xia^{1,2}, *Dehong Chen*³, *Nicola V. Y. Scarlett*², *Ian C. Madsen*²,
*Matteo Leoni*⁴, *Deborah Lau*¹, and *Rachel A. Caruso*^{1,3}

¹CSIRO Materials Science and Engineering, Clayton, VIC 3168, Australia; ²CSIRO Process Science and Engineering, Clayton, VIC 3168, Australia; ³PFPC, School of Chemistry, The University of Melbourne, Melbourne, VIC 3010, Australia; ⁴Department of Civil, Environmental and Mechanical Engineering, University of Trento, 38123 via Mesiano 77, Trento, Italy.

fang.xia@csiro.au

Mesoporous anatase (TiO₂) beads are superior electrode materials for high performance dye-sensitized solar cells, producing greater than 10% solar to electric power conversion efficiency. Efficient solvothermal synthesis routes for mesoporous anatase beads may be developed by better understanding the reaction mechanism and kinetics. In this study, a series of *in situ* and time resolved X-ray diffraction (XRD) experiments have been conducted at the Australian Synchrotron. The solvothermal syntheses were conducted in quartz glass capillary microreactors while diffraction patterns were collected every 1-2 min. This allowed the induction period and the rate of crystallization from amorphous precursor to anatase to be determined for various synthesis conditions. This poster presentation describes the effects of time, temperature, precursor size and type (with or without hexadecylamine), and solution composition on the reaction kinetics, as well as on the domain size, size distribution, and morphology. Based on the kinetic evidence and post microscopic examination, we conclude that the synthesis follows a 3-dimensional bulk crystallization mechanism. The kinetics also shows promise for rapid and large scale production.

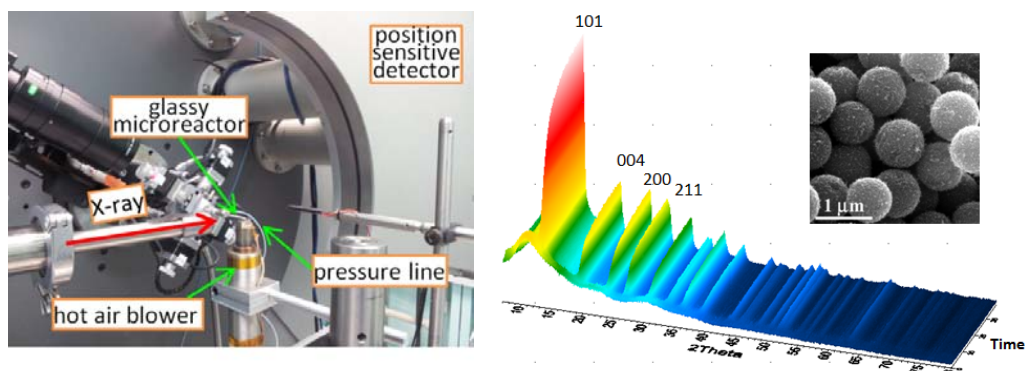


Figure: (left) experimental setup; (right) *In situ* synchrotron XRD patterns showing the progressive growth of mesoporous TiO₂ beads from the amorphous precursor during solvothermal synthesis at 160 °C.

Structure Determination of a New Interrupted Zeolite PKU-14 by Combining Powder X-ray Diffraction, Rotation Electron Diffraction, NMR and IR Spectroscopy

Jie Su¹, Jie Liang², Yingxia Wang^{2*}, A. Ken Inge¹, Junliang Sun^{1,2}, Xiaodong Zou¹, Jianhua Lin^{2*}

¹Berzelii Centre EXSELENT on Porous Materials, and Department of Materials and Environmental Chemistry, Stockholm University, Stockholm, Sweden

²College of Chemistry and Molecular Engineering, Peking University, Beijing, China
jie.su@mmk.su.se

By combining powder X-ray diffraction, rotation electron diffraction (RED), NMR and IR spectroscopy, a new interrupted zeolite PKU-14 was solved. The ¹⁹F NMR spectrum suggests D4R units exist in the structure. The IR spectrum of PKU-14 shows some similarity with that of ASU-7 within the range 400-1000 cm⁻¹, which may reveal PKU-14 could be a zeolitic structure. However, the stretching vibrations of -OH groups at about 3500 cm⁻¹ indicates that the structure might be an interrupted zeolite. The three-dimensional reciprocal lattice PKU-14 was reconstructed from the RED data, and from which the unit cell was determined to be $a=19.058 \text{ \AA}$, $b=19.039 \text{ \AA}$, $c=27.365 \text{ \AA}$, $\alpha=89.89^\circ$, $\beta=89.97^\circ$, $\gamma=89.62^\circ$ using the RED software package[1]. From the reflection conditions, it indicates that the possible space group could be $I4cm$, $I-4c2$, $I4/mcm$. Because more than 90% of the zeolite crystal structures in the IZA database are centrosymmetric, most attention was paid to space group $I4/mcm$. Finally, the structure was solved by using powder X-ray diffraction data with a simulated annealing parallel tempering algorithm using the program FOX[2]. The structure is built by the $[4^66^{12}]$ cages interconnected with D4R units. ITQ-21[3] and ITQ-26[4] are also built by the similar building units, but with a 4MR segment inside the $[4^66^{12}]$ cage. In PKU-14, all the terminal hydroxyl groups point to centre of the $[4^66^{12}]$ cage, but there is no additional species inside it. Therefore, PKU-14 can be considered as a defective structure of ITQ-21 or ITQ-26. Similar to ITQ-21 and ITQ-26, PKU-14 also shows a three-dimensional 12MR channel system.

References

- [1] D. L. Zhang, P. Oleynikov, S. Hovmöller, X. D. Zou, *Kristallogr.* 225(2010) 94–102.
- [2] V. Favre-Nicolin, R. Černý, *J. Appl. Cryst.* 35(2002) 734-743.
- [3] A. Corma, M. J. Díaz-Cabañas, J. Martínez-Triguero, F. Rey, J. Rius, *Nature* 418(2002) 514-517.
- [4] D. L. Dorset, K. G. Strohmaier, C. E. Klierer, A. Corma, M. J. Díaz-Cabañas, F. Rey, C. J. Gilmore, *Chem. Mater.* 20(2008) 5325–5331.

Formation Mechanisms of Complex Ca-rich Ferrite Iron Ore Sinter Bonding Phases

*Nathan A.S. Webster^{1,2}, Mark I. Pownceby¹,
Ian C. Madsen¹, and Justin A. Kimpton³*

¹CSIRO Process Science and Engineering, Box 312, Clayton South, VIC, 3169, Australia

²Australian Nuclear Science and Technology Organisation, Locked Bag 2001, Kirrawee DC, NSW, 2232, Australia

³Australian Synchrotron, 800 Blackburn Rd. Clayton, VIC, 3168, Australia
nathan.webster@csiro.au

Iron ore sinter, a composite material comprised of iron ore fines bonded by a matrix of complex Ca-rich ferrite phases, is a major component of blast furnace feed material. Most of the Ca-rich ferrites contain silica and alumina and are known collectively by the acronym 'SFCA' (Silico-ferrite of Calcium and Aluminium), and these SFCA phases impart desirable physical properties of high strength, high reducibility and low reduction degradation to iron ore sinter. Despite their importance in controlling the quality of iron ore sinter, however, a deep fundamental understanding of the formation of SFCA phases from precursor phases, and the impact of parameters such as temperature, chemical composition and oxygen partial pressure, does not exist.

Through an *in situ* X-ray diffraction-based experimental program, executed on the powder diffraction beamline at the Australian Synchrotron^[1], and also on a laboratory INEL diffractometer, significant new insights into the formation of SFCA phases under simulated sintering conditions have been obtained^[2,3,4]. This includes the observation and subsequent characterisation of several phases previously unknown in the context of iron ore sintering, but which are critical to the formation of the SFCA phases during both solid state phase formation during heating and crystallisation from melt phases during cooling. It also includes determination, via Rietveld refinement-based quantitative phase analysis, of the effect of the various sintering parameters on the amounts of the SFCA phases formed. This presentation will outline the experimental, data collection and data analysis methodologies designed to provide a deep understanding of the SFCA phase formation mechanisms, with the ultimate aim of this research being to provide industry with the knowledge to consistently produce high quality sinter despite highly variable physical and chemical characteristics of the ore material.

References

[1] Beamtime awards AS093/PD1639 and AS113/PD4160.

[2] Nathan A.S. Webster *et al.*, *Metall. Mater. Trans. B*, 2013, 1344-1357.

[3] Nathan A.S. Webster *et al.*, *ISIJ Int.*, 2013, in press.

[4] Nathan A.S. Webster *et al.*, *ISIJ Int.*, 2013, submitted.

Structural Phase Transition and Thermal Expansion in $\text{Bi}_{1-2.5x}\text{Pr}_{1.5x}\text{Ba}_x\text{FeO}_3$ $x=0.05,0.1$ Ceramics

G. F. Cheng, Y. J. Ruan, Y. H. Huang, X. S. Wu

Analysis & Testing Center for Inorganic Materials, Shanghai Institute of Ceramics, Chinese Academy of Sciences gfcheng@mail.sic.ac.cn

The temperature dependence of the crystal structure for $\text{Bi}_{1-2.5x}\text{Pr}_{1.5x}\text{Ba}_x\text{FeO}_3$ ($x=0.05,0.1$) polycrystallines is studied by X-ray powder diffraction with Rietveld refinements in the temperature range of 25-800°C. A structural phase transition of Rhombohedral-to-Cubic occurs for $\text{Bi}_{0.875}\text{Pr}_{0.075}\text{Ba}_{0.05}\text{FeO}_3$ sample in the temperature of 600-700°C, which may relate to its unstable rhombohedra distorted structure with the space group $R3c$. The rarely decomposition of these samples indicates that the Pr, Ba co-doped make the BiFeO_3 ceramics more stable. The thermal expansion determined by the temperature dependence of the unit-cell lattice parameters and volumes for $\text{Bi}_{1-2.5x}\text{Pr}_{1.5x}\text{Ba}_x\text{FeO}_3$ samples is also investigated, which shows an isotropic and positive behavior. The average thermal expansion coefficient decreases with the increasing x . We argue that the cubic crystal structure with the high symmetrical of the space group $Pm3m$ may be more stable for $\text{Bi}_{0.75}\text{Pr}_{0.15}\text{Ba}_{0.1}\text{FeO}_3$ sample, which may explain the reason why no phase transition occurs and its lower thermal expansion efficiencies. An obvious change in the slope of the linear fitted lines between 300°C and 400°C suggests a possible antiferromagnetic-paramagnetic transition, which occurs around the Néel temperature of the $\text{Bi}_{1-2.5x}\text{Pr}_{1.5x}\text{Ba}_x\text{FeO}_3$ samples.

Structural Refinements From Multiple Measurement Techniques Using a Reverse Monte Carlo Method

Victor Krayzman and Igor Levin

Materials Measurement Science Division, National Institute of Standards and Technology,
Gaithersburg MD 20899, igor.levin@nist.gov

A Reverse Monte Carlo (RMC) method enables explicit determination of local and mesoscale atomic order/displacements in polycrystalline bulk and nanostructured materials, including solid solutions. This method employs large atomic configurations, where the coordinates of individual atoms are treated as variables to fit the data. Yet, with the number of structural variables reaching the tens of thousands, overfitting becomes the primary issue. The RMCProfile software allows for simultaneous fitting of the total scattering data and Bragg intensities, thereby providing constraints on the average structure. Additionally, this software incorporates a suite of geometric and bond-valence-sum restraints. However, our experience has demonstrated that with complex structures the powder diffraction data are frequently insufficient for obtaining the correct solutions. Worse than that, the application of restraints can lead to seemingly sound but erroneous structural models. To address this problem, we have extended the RMCProfile software to enable the *simultaneous* fitting of not only neutron/X-ray total scattering and Bragg intensities, but also of XAFS data and patterns of diffuse scattering in single-crystal diffraction. In this presentation, we will demonstrate the results of such combined analyses for the BaTiO₃-based ferroelectrics. We will show that multiple-technique RMC refinements provide access to key structural features with the detail and accuracy inaccessible by any other method. In electronic ceramics, these fine structural features control the functional response of the material.

Rapid and Accurate Calculation of Scattering Profiles Using the Golden Ratio

Max C. Watson and Joseph E. Curtis

NIST Center for Neutron Research, max.watson@nist.gov

Calculating the scattering intensity of an N -atom system is a numerically exhausting $O(N^2)$ task. We present a simple approximation technique that scales linearly with the number of atoms. Using an exact expression for the scattering intensity $I(\mathbf{q})$ at a given wave vector \mathbf{q} , we compute the rotationally averaged intensity $I(q)$ by evaluating $I(\mathbf{q})$ in several scattering directions. The orientations of the \mathbf{q} -vectors are taken from a quasi-uniform spherical grid generated by the golden ratio. This technique is fully general, allowing for arbitrary collections of scattering lengths and atomic positions. The processing time scales sub-linearly in N when the atoms are identical and lie on a lattice. The procedure is easily implemented and should accelerate the analysis scattering data.

Proficiency Test Program for Quantitative X-Ray Powder Diffraction Analysis of Portland Cements

Paul Stutzman

National Institute of Standards and Technology,
100 Bureau Dr. Gaithersburg, MD 20899-8523, USA Paul.Stutzman@NIST.gov

Quantitative X-ray powder diffraction analysis is increasingly used within the portland cement industry. However, ASTM C1365, standard test method for powder diffraction analysis of cements, does not provide an explicit method for quantifying phase concentration. The standard utilizes qualification criteria, where analyses of a set of certified reference materials must fall within stated precision and bias limits based upon an inter-laboratory study. Validation of X-ray powder diffraction analyses by the Rietveld method is particularly important because the normalization inherent in the mass fraction calculations can obscure bias. A set of portland cements were distributed to 29 laboratories for analysis according to the labs' individual protocols. The results are presented graphically with Youden plots which incorporate ranking to illustrate relative lab precision and bias based upon a consensus mean for each phase and ASTM C1365 performance qualification criteria. In practice, labs that fall outside of the compliance limits would be provided with information via the Youden plots to help assess their systematic and random error. Proficiency testing of this sort provides participating laboratories with a quantitative assessment of their performance relative to peers and evaluation of their performance against current standard test qualification criteria. Such a quantitative assessment could be used to qualify laboratories and may be stipulated in a specification.

High(er) Accuracy in Structure Determination of Organic Compounds Using MYTHEN 24K Detector

Dubravka Šišak Jung

DECTRIS Ltd. dubravka.sisak@dectris.com

Choice of the method for structure determination from X-ray powder diffraction (XPD) data depends on the investigated material, the radiation used, data quality and prior knowledge about the material. In most cases, XPD patterns of organic compounds are of low resolution (radiation damage, light atoms), so structure determination is commonly carried out by direct space methods. However, in some cases ab initio structure determination is necessary. These methods usually require high resolution data and reliable intensities.

In this work, ab initio structure analysis of several organic compounds was carried out using the data measured with the MYTHEN detector, installed at the SLS synchrotron facility. These high quality data are result of: (1) complete angle range (120°) is measured simultaneously, so no discrepancy between low and high angles is present. (2) the exposure time is short, so several patterns are consecutively measured. These can be processed individually (time resolved experiments) or averaged to obtain better data statistics. As only similar (same) patterns are averaged, the resulting pattern is more precise. (3) low noise level enables the reflection intensities to be determined more accurately.

Structure analysis of two polycrystalline samples (TY-120, cyclo- β -peptide, and TY-207, co-crystal) was hindered by the lack of molecular model, poor statistics (TY-120) and radiation damage (TY-207). Both structures were solved by using averaged (carefully chosen) XPD patterns, and charge flipping algorithm. Subsequent Rietveld refinement of structure TY-120 could be performed without geometrical restraints, proving that the model is correct. Refinement of TY-207 structure revealed fine details, such as disorder of chlorine atoms.

Structure of D-ribose was determined by combination of direct space algorithm and series of Fourier syntheses. This resulted not only in the correct structure, but also disorder of hydroxyl groups could be accurately described. It is found to comply with NMR results. Structure of D-mannose was solved from single crystal data, but the final model lacked some atoms, and some Uaniso were negative. Such model was refined with the high resolution MYTHEN data. Refinement without geometrical restraints proved to be exceptionally stable. Moreover, examination of difference Fourier maps revealed disordered hydroxyl group.

These results are part of the PhD work carried out in Laboratory for Crystallography, ETH Zurich, under supervision of Dr. L.B. McCusker and Dr. Ch. Baerlocher

Structure Solution of Cocrystals of Ketoconazole from Powder Data

Stephan X.M. Boerrigter^{1,2} and Andrew Otte²

1) SSCI, a Division of Aptuit, West Lafayette, IN 47906

2) Industrial and Physical Pharmacy, Purdue University, West Lafayette, IN 47907
steef.boerrigter@aptuit.com

Cocrystals of the antifungal drug ketoconazole were grown from 4 dicarboxylic acids: adipic, succinic, fumaric, and oxalic acid. All formed 1:1 crystalline single phases. The powders were analyzed using synchrotron radiation through the 11-BM mail-in program at Argonne National Laboratory.

The structures were elucidated using two alternative approaches, one using DASH with subsequent rigid body refinement in TOPAS, one using FOX with subsequent refinement in TOPAS using MOGUL-derived restraints. Comparable structures were obtained for all but the ketoconazole–fumaric acid cocrystal. DASH produced a more chemically intuitive hydrogen bonding motif than that of the FOX sampling. When the DASH solution—initially refined using the rigid body approach—was further refined using the MOGUL-derived restraint model, the hydrogen bonding motif interestingly collapsed to become more similar to that of the FOX approach.

In general, we believe the FOX default restraint sampling method offers little advantage over the rigid body with flexible torsion angles approach of DASH. The FOX final least-squares fits appear to produce less realistic molecular conformations and less intuitive hydrogen bonding motifs for these particular molecular systems. TOPAS sampling was not able to solve these structures; at least not within a similar time span that FOX and DASH could.

Structure refinement in TOPAS is clearly superior to the least-squares refinements of FOX and DASH, but for these molecular systems it is necessary to apply an advanced molecular model to obtain realistic results. A rigid-body approach with flexible torsion angles produced weighted fit residuals in the order 12–16%, whereas a restraint model based on MOGUL statistics and riding hydrogen atoms resulted in fit residuals in the order 6–8%. However, setting up the TOPAS input files for this approach is a labor-intensive endeavor.

Crystal Structures of $\text{SrR}_2\text{Sc}_2\text{O}_7$, R = Pr, Nd, Sm, Eu, and Gd

James A. Kaduk

Illinois Institute of Technology, Chicago IL 60616

kaduk@polycrystallography.com

The crystal structures of these compounds were reported (Titov *et al.*, 2009) in *Immm*, based on laboratory X-ray powder diffraction data. Our laboratory data indicated that the symmetry was lower, so we collected synchrotron powder data at beam line 11-BM at the Advanced Photon Source at Argonne National Laboratory, to characterize the distortions from the reported structure.

These compounds crystallize in *Pnma*, with lattice parameters in the ranges: $5.722 < a < 5.724$, $19.995 < b < 20.317$, $5.708 < c < 5.770$ Å, and $655.661 < V < 671.502$ Å³. Although the lattice parameters increase with the size of the lanthanide cation, the increase is not linear. Although the metal atoms have a high-symmetry arrangement, the oxygen polyhedra are distorted and tilted from the arrangement originally reported. The Sc sites are 6-coordinate (octahedral), and are occupied only by Sc. The R sites are 7-coordinate (considering R-O distances < 3.0 Å), except for Gd, which is 6-coordinate. For the larger lanthanides, both the Sr and R sites exhibit partial occupancy by the other large cation. As the lanthanide gets smaller, the site occupancies become closer to stoichiometric; in $\text{SrGd}_2\text{Sc}_2\text{O}_7$ the site occupancies are all unity. The anisotropic strain broadening is more complex than can be described using the normal tensor model; conclusions about the microstructure will be discussed. A density-functional geometry optimization of the Gd compound yielded excellent agreement with the refined structure, and provides insight into the bonding in these compounds.

References

Yu. A. Titov, N. M. Belyanina, V. Ya. Markiv, M. S. Slobodyanik, Ya. A. Krayevska, and V. V. Chumak, *Dopov. Nats. Akad. Ukr.*, 155-161 (2009).

Real Space Models to Quantify Stacking Disorder in Topochemically-Converted Layered Oxides

Scott T. Misture

Kazuo Inamori School of Engineering, Alfred University
misture@alfred.edu

$\text{Bi}_2\text{NaCaNb}_3\text{O}_{12}$ (BCNN) is an Aurivillius phase with $[\text{Bi}_2\text{O}_2]^{2+}$ sheets interleaved between perovskite-like layers. Topochemical conversion to the protonated form may be achieved using simple acid treatment that removes the $[\text{Bi}_2\text{O}_2]^{2+}$ sheets, protonates the perovskite sheet surfaces, and introduces interlayer water. Protonated BCNN nanosheet suspensions demonstrate remarkably high photocatalytic activity for water splitting to produce H_2 , but the structural and electronic origins of this remarkable materials property remain unknown.

Powder XRD data for protonated BCNN suggest stacking disorder that differs from turbostratic disorder. Multiple models were used to fit the XRD data. Of these, only models which allow incommensurate shifts along the *a-b* plane of the perovskite sheets, along with varied interlayer spacings, can successfully describe the data.

Modeling was undertaken using the software *TOPAS* (Bruker-AXS) by incorporating rigid bodies into supercells of 2, 4, 6, 8, 12, 18, and 36 units along the *c*-axis stacking direction. Two structure models were incorporated: one with the orthorhombic symmetry that is present in the parent Aurivillius phase and a second that assumes some relaxation during the topochemical conversion to tetragonal symmetry.

Following earlier work, an aperiodic model with one layer represented by a rigid body in a 12-unit supercell was successfully applied to simulate the non-basal reflections. Excellent fitting was also achieved using filled supercell models that simulate all *hkl* peaks in a single simulation, with up to 1050 atoms in the filled 36-layer supercell. The calculation time for even the most complex refinement of 36-layer supercells with a *c*-axis length of 502Å was shorter than 5 minutes.

In order to probe structure relaxations of the individual perovskite layers that might occur during topochemical conversions, we defined the rigid body in the context of a unit cell, rather than as a *z*-matrix or using Cartesian coordinates. Refinement of the subcell lattice parameters concurrently with the supercell dimensions then gives a first indication of relaxations.

Optimized models show that the interlayer shifts between successive perovskite blocks are centered on the expected commensurate value (0.25 along *a*- and *b*-axes) but with a broad distribution. Likewise, the absolute interlayer spacings show a broad distribution, ranging from 1.80 to 4.13Å, with an average value of 2.37(53)Å, yielding physically-reasonable oxygen-oxygen distances. On average, one H_2O per formula unit can be accommodated in the interlayer galleries in the superstructure model, but again with a wide distribution from layer to layer. The method allows quantification of small but statistically significant relaxations of the perovskite sheets. We find that the distortions present in the parent

Aurivillius phase remain largely intact in the nanosheets, yielding internal electric fields that may enhance charge separation in the photoreaction.

“Morse” Restraints: A New Approach to Rietveld-Refined Structure Verification

I. S. Bushmarinov and A. O. Dmitrienko

A.N. Nesmeyanov Institute of Organoelement Compounds RAS,
Moscow, Russia ib@ineos.ac.ru

Despite the current progress in structure solution and refinement from powder data, this process cannot be yet considered trivial and error-proof for organic molecules. The organic structures are usually solved from powder data using a Monte-Carlo search in direct space, and this search provides a number of possible crystal structures. Due to limitations of this approach, the “best” solution can still correspond to a non-existent crystal structure. Moreover, the Monte-Carlo search requires a starting model, which is usually deduced from synthetic and/or spectral information, and can e.g. correspond to a wrong isomer. In this case, the search in direct space can still provide reasonably looking results.

The typical Rietveld refinement, at the same time, lacks unambiguous criteria for detection of wrong structures, as has been demonstrated for γ -quinacridone: a completely wrong structure proposed for it was refined against a poor dataset and demonstrated to be “acceptable”.

In our study, we provide a new approach to verification of Rietveld-refined structures by introducing a new restraint scheme for Rietveld refinement based on Morse bond energy potential is introduced, in which the asymmetry of Morse potential allows the refinement to “break” the incorrectly-placed bonds [1]. The analysis of bond length distributions in models refined using these “Morse” restraints at different values of restraint strength is then performed. It reveals a visible difference in behavior of wrong and correct structures: the bond length distribution in wrong structures contains outliers, which can be determined using robust statistical methods. The absence of such outliers becomes a criterion of structure correctness. This approach is implemented in TOPAS macro language and can be used both for refinement and for verification of crystal structures, increasing their accuracy without requiring any additional data or calculations.

Our approach was tested on the known difficult cases of γ -chinacridone an quinacridone and used for the Rietveld refinement of $\text{Ph}(\text{CH}_2)_5\text{C}(\text{O})\text{-Gly-L-Trp-NH}_2$, an organic molecule of a potential anxiolytic containing 32 non-hydrogen atoms and 14 single bonds [1]. In all cases, the wrong structure model could be easily distinguished from the right one. The applicability of the proposed approach was also demonstrated on several smaller organic and organometallic structures.

References

- [1] I.S. Bushmarinov, A.O. Dmitrienko, A.A. Korlyukov, M.Yu. Antipin, *J. Appl. Cryst.* 45 (2012) 1187–1197.

Accurate Low-Angle Measurements With a Focusing Mirror

Martijn Fransen, Detlef Beckers and Joerg Bolze

PANalytical, Lelyweg 1, 7602 EA Almelo, The Netherlands

martijn.fransen@panalytical.com

Measuring accurate peak positions at 2θ angles below 10 degrees is generally difficult in the commonly used reflection geometry. The incident beam has to be slit down in order to avoid overirradiation of the sample, causing a loss in intensity, and the peak position becomes extremely sensitive to sample preparation and positioning in the diffractometer.

With transmission geometry, these issues can be solved. A larger portion of the X-ray beam can be used, and the geometry is much less sensitive to sample positioning errors at low angles. Transmission diffractometers used to be dedicated instruments, however, and reconfiguring them to reflection geometry is not easy. In the last years, we have started to use X-ray mirrors with an elliptical shape for transmission geometry. These mirrors are designed to focus the divergent beam from the source onto the goniometer circle and can be easily changed for divergence slits when measurements in reflection geometry are desired. Elliptical mirrors have a clear advantage over mirrors of parabolic shape – with the latter, the resolution directly depends on the beam size, which makes them unattractive for transmission powder work.

With focusing mirrors, accurate, high intensity peaks can be obtained at angles as low as 0.1 degrees 2θ . This makes the focusing mirror ideal for e.g. nanostructured materials, proteins and pharmaceutical substances, to name a few. Examples from these materials will be shown.

Accurate Variable-Temperature Measurements with Furnace-Type Non-Ambient Chambers

M. Fransen¹, Ch. Resch² and G. Artioli³

¹PANalytical B.V., Lelyweg 1, 7602 EA Almelo, The Netherlands, ²Anton Paar GmbH, Graz, Austria, ³University of Padova (formerly University of Milano), Italy
martijn.fransen@panalytical.com

In the last decade, the furnace-type non-ambient chamber has largely replaced the traditional strip heater for non-ambient experiments up to about 1200 °C. In these furnace heaters, the sample is mounted on a long pole, and is loaded from the bottom of the chamber. The advantages of furnace heaters are manifold: 1) the temperature of the sample is much more uniform than in strip heaters, 2) it is possible to spin the sample, and 3) it is much easier to avoid reactions between the sample and the holder.

A disadvantage of furnace heaters is that the pole on which the sample is mounted will expand as a function of temperature, on the order of a few tenth of mm. The resulting changes in peak positions in the diffractogram will be a combination of lattice parameter changes (wanted) and sample position errors (unwanted).

Parallel beam geometry (a parabolic X-ray mirror in the incident beam and an equatorial collimator in the diffracted beam) instead of the normally used Bragg-Brentano focusing geometry is a possible way out for this problem. This geometry is insensitive for sample position variations and the true peak shifts from lattice parameter changes are directly visible. With this geometry however, it is much more difficult to obtain a high resolving power in 2Theta (determined by the equatorial collimator) making this geometry slow.

We have developed a different solution, in which the changes in sample position as a function of temperature are automatically compensated. With this method, normal focusing geometry can be used again, and the peaks shifts resulting from lattice parameter changes are directly visible. A prototype solution has been working well in the laboratory of one of us (G.A.) for several years, and it has now also been implemented on commercially available diffractometers. In this contribution, we explain the methodology in more detail and show its benefits with application examples.

Accuracy Evaluation of Commercial X-Ray Powder Diffractometers Using NIST Standards

*F. González^a, X. Bokhim^b, J. Miranda^b, E. Barrera-Calva^a,
A. Tejeda^c and R. López-Juárez^d*

^aLaboratorio de rayos X de la División de Ciencias Básicas e Ingeniería-Departamento de Ingeniería de Procesos e Hidráulica, Universidad Autónoma Metropolitana-Iztapalapa, A.P. 55-534, 09340 México D.F., Mexico. ^bInstituto de Física, Universidad Nacional Autónoma de México, A.P. 20-364, 01000 México D.F., Mexico. ^cInstituto de Investigaciones en Materiales, Universidad Nacional Autónoma de México, A.P. 70-360, México D.F., Mexico. ^dCentro de Ciencias Aplicadas y Desarrollo Tecnológico, Universidad Nacional Autónoma de México, A.P. 70-186, México D.F., Mexico. fgg@xanum.uam.mx

The influence of the experimental arrangement on the accuracy in X-ray powder diffraction is a key issue for the quantitative analysis of measured data. In this work, we present an analysis of the accuracy for experimental arrangements in six different diffractometers. In order to have a robust analysis to assess the accuracy and reproducibility, we have performed long and high counting rate measurements for the NIST standards SRM660b (LaB₆) and SRM1976b (Al₂O₃). The geometry, with one exception, was Bragg-Brentano, with different source-sample-detector distances for all the arrangements. In most experiments, X-ray source was a tube with Cu anode, and the detector was linear-type. A first round of measurements was performed in the instruments under normal operating conditions. Whenever possible, a second round was carried out after the calibration. The measured data were analyzed by following the procedures reported in the certificates for the standards SRM 660b and SRM 1976b [1, 2], by using a fundamental parameters approach during the Rietveld refinement. The Cu K α X-ray emission profile was modeled with the one reported by G. Hölzer et al. [3]. The refined parameters included polynomial terms for modeling of the background, the lattice parameters, terms indicating the position and intensity of the “tube tails” (if possible, they were measured), specimen displacement, structural parameters, preferred orientation, and the width of a Lorentzian profile for modeling the average crystallite size.

Acknowledgements: We thank CONACyT-México for financial support, project INFR-2011-1-163250, and LDRX (T-128) UAM-I, LRX IIM-UNAM and LAREC IF-UNAM for the XRD measurements.

References

- [1] Certificate of Standard Reference Material 660b (2010);
- [2] Certificate of Analysis of Standard Reference Material 1976b (2012). National Institute of Standards and Technology; U.S. Department of Commerce: Gaithersburg, MD, .USA.
- [3] G. Hoelzer, et al. *Phys. Rev.* **56**, 4554 (1997).

Are Your Bragg Peaks Sharp Enough Now? (Understanding Accuracy Challenges in High-Resolution Synchrotron Powder Diffraction)

Matthew R. Suchomel, Lynn Ribaud,
Robert B. Von Dreele, and Brian H. Toby*

Advanced Photon Source, Argonne National Laboratory, Argonne, IL

* suchomel@aps.anl.gov

Synchrotrons have revolutionized powder diffraction. They make possible the rapid collection of data with tremendous angular resolution and exceptional signal to noise ratios. The high penetration and wide Q range afforded by high energy light sources like the Advanced Photon Source (APS) even allows synchrotrons to make inroads into territory that previously demanded neutron scattering techniques. High resolution beamlines (such as 11-BM at the APS) employing multiple bank single crystal analyzer detectors routinely reveal subtle crystallographic distortions undetectable on other powder instruments, and enable structure solution from powder data for increasingly complex materials with superb discrimination of individual Bragg peak reflections.

Beamline 11-BM at the APS is a dedicated high resolution ($\Delta Q/Q \sim 2 \times 10^{-4}$) powder diffraction instrument which uses vertical and horizontal beam focusing capabilities and a counting system consisting of twelve perfect crystal analyzers paired with scintillator detectors. It supports both traditional on-site experiments and a highly successfully rapid access mail-in access mode. This mail-in mode has greatly simplified access to world-class synchrotron quality powder data for a large number of users (> 200 in 2012). However, the seemingly simple text data files presented to the end user (2θ position and scattering intensity, plus sigma) mask many involved alignment, calibration, correction and merging routines needed to efficiently and accurately reduce the numerous multi-bank detector datasets associated with a high throughput user program.

This presentation will highlight current and planned details of data reduction at 11-BM, particularly as applied to ensuring accurate and consistent high quality data for a high-throughput measurement access model. In particular, ongoing efforts to automate a correction for small mechanical 2θ precision errors ($< 0.0005^\circ$) will be discussed. Examples illustrating how this often overlooked correction can result in quantitative improvements to the accuracy of the reduced high-resolution powder diffraction data will be presented; as demonstrated by superior Rietveld fits, improved pattern indexing, and more effective attempts at structure solution.

A Thermal Neutron TOF Powder Diffractometer Concept for the ESS

*Paul Henry¹, Britt Rosendahl Hansen^{2,4}, Sonja Lindahl Holm^{3,4},
Kim Lefmann^{3,4}*

¹ESS AB, Lund, Sweden, ²DTU Physics at the Technical University of Denmark, Denmark, ³Niels Bohr Institute, University of Copenhagen, Denmark, ⁴ESS Design Update Programme – Denmark. paul.henry@esss.se

The thermal neutron instrument concept is a t-o-f diffractometer with variable wavelength resolution ($\Delta\lambda/\lambda$ from 0.02 % to 5 % for a λ_{mean} of 1.45 Å), provided by a pulse shaping chopper. It will have a useful Q_{max} of approximately 25 Å⁻¹ for medium and high-resolution powder crystallography. The usable wavelength band in the time-frame is 1.9 Å (normal operational mode $\lambda = 0.5 - 2.4$ Å) and the instrument beam transport system is optimised for shorter wavelengths for structural characterisation and *in situ* processing. The ability to tune the instrument resolution to the experiment requirements is a major advantage of ESS instruments. The combination of the very flexible instrument set-up, event-mode data acquisition and optimised sample environments are key to the impact of this instrument across a broad range of science. While the instrument will be optimised for thermal neutron powder diffraction, it will also be possible to perform single crystal diffraction measurements in a quasi-Laue mode or to use longer wavelength bands.

The ESS is a European large-scale facility project with 17 international partners based in Lund, Sweden. It is scheduled to deliver its first neutrons to target in 2019 and have its full design complement of 22 public instruments by 2025. The ESS will offer new opportunities to all areas of scientific research, as well as complementing the existing neutron sources, both reactor and spallation-based, in Europe. The instrument suite is currently under development and provides an opportunity to investigate and evaluate novel instrument concepts that fully utilise the possibilities presented by a long-pulse source.

The Pulsed Monochromatic Powder Diffractometer Concept for the ESS

Paul F. Henry

ESS AB, Lund, Sweden paul.henry@esss.se

Powder diffraction is the cornerstone of materials characterisation, determining where atoms are in space, without which it would be impossible to relate structure to physical properties. Neutron powder diffraction is highly complementary with X-ray powder diffraction for structure determination and refinement. Reflecting on neutron powder diffraction instrumentation over the last 40 years, a clear trend emerges in instrument types built at large scale facilities. Reactor-based neutron instruments are predominantly based on crystal monochromators and at spallation sources on the wide wavelength band time-of-flight (t-o-f) technique. Is this the only way to build instruments or has it just become the accepted way? Here, I discuss the pros and cons of building a crystal monochromator-based neutron powder diffractometer at a long-pulse spallation source and the new experiment types that would become possible compared with existing instruments.

The ESS is a European large-scale facility project with 17 international partners based in Lund, Sweden. It is scheduled to deliver its first neutrons to target in 2019 and have its full design complement of 22 public instruments by 2025. The ESS will offer new opportunities to all areas of scientific research, as well as complementing the existing neutron sources, both reactor and spallation-based, in Europe. The instrument suite is currently under development and provides an opportunity to investigate and evaluate novel instrument concepts that fully utilise the possibilities presented by a long-pulse source.

PLSR (as Full Pattern Approach) or, Why We Sometimes Can Simply Forget About Profile Shapes

T. Degen¹, U. Koenig¹, D. Beckers¹, D. Stauch-Steffens²

¹PANalytical B.V., Almelo, The Netherlands, ²University of Bonn, Germany
thomas.degen@panalytical.com

Usually in XRPD we are paying lots of attention to accurately describe profile shapes. We do that to eventually extract/predict information from the full pattern using physical models and fitting techniques. Sometimes this approach is stretched to its limits. That usually happens, when no realistic physical model is available, or when the model is either too complex or doesn't fit to reality.

In such cases there is one very elegant way out: multivariate statistics and **Partial Least-Squares Regression**. This technique is rather popular in spectroscopy as well as in a number of science fields like biosciences, proteomics and social sciences.

PLSR as developed by Herman Wold [1] in 1960 is able to predict any defined property Y directly from the variability in a data matrix X. In the XRPD the rows of the data matrix used for calibration are formed by the individual scans and the columns are formed by all measured data points.

PLSR is particularly well-suited when the matrix of predictors has more variables than observations, and when there exists multi-collinearity among X values. In fact with PLSR we have a full pattern approach that totally dismisses profile shapes but still uses the complete information present in our XRPD data sets.

We will show a number of cases where PLSR was used to easily and precisely predict properties like crystallinity and more from XRPD data.

References

[1] Wold, H. (1966). Estimation of principal components and related models by iterative least squares. In P.R. Krishnaiah (Ed.). *Multivariate Analysis*. (pp.391-420) New York: Academic Press.